Mechanics of Advanced Composite Structures 9 (2022) 37 – 47

Semnan University

Mechanics of Advanced Composite Structures

journal homepage: http://MACS.journals.semnan.ac.ir

Simulation and Optimization of Fatigue Life of Carbon-Epoxy Composite Sub Frame

R. Talebitooti [a*], S.M. Seyedraoufi [b]

[a] *Department of Mechanical Engineering, Iran University of Science and Technology, Tehran, Iran*
[b] *Automotive Engineering, Iran University of Science and Technology, Tehran, Iran*

KEYWORDS

Fatigue;
Sub-frame;
Composite;
Epoxy-Carbon;
Optimization.

ABSTRACT

Recently, automotive companies are interested in the usage of composite materials, because of their mechanical properties such as high strength-to-weight ratio, high stiffness, and flexibility in layout configurations. In the present work, fatigue failure was determined based on Lessard and Shokrieh progressive model in composite sub-frame subjected to fatigue loading in its service life, and a genetic algorithm was used to find the optimum stacking sequence to achieve maximum fatigue life. According to the results, $[\pm 45_4/0_{12}]_s$ laminate was determined as the optimum orientation. Since the simulation results have shown usage of 90◦ layers as consecutive plies end up a progression of matrix damage and increase of stress while using ±45◦ layers as outer layers lead to increase the stiffness, toughness, and impact resistance of laminate and postpone the failure in laminate. It can be seen that the elements failed in matrix and delamination modes around 40% and 50% of total life, respectively. Moreover, before catastrophic failure, 7%, 8.55%, and 13% degradation happened in longitudinal, transverse, and shear stiffness respectively. Like wisely, 20%, 23%, and 46% degradation occurred in longitudinal, transverse, and shear strength discretely.

1. Introduction

Recently, manufacturers are encouraged to reduce the weight of vehicles as global competition in the automotive industry to produce safe vehicles with low fuel consumption. On the other hand, weight loss of metal parts leads to a reduction of mechanical properties, accordingly, polymer-based composites such as epoxy-carbon composite are good alternatives in a structure of vehicle due to benefits of high stiffness and strength, good chemical resistance, and low weight. Also, composites provide considerable flexibility in design which allows changing material systems in various ways.

Franz et al. [1] researched about effects of laminate thickness on the behavior of FRP composite. They proposed a new procedure to regard uncertainties in ply thickness on FRP composites with an optimized fiber layout. For this intent, sensitivity analysis was taken place to inquire significance of parameters on structural behavior. By considering this issue, producers could discern critical and non-critical laminate parameters in their production process.

Tyflopoulos et al. [2] optimized the topology and fiber direction of a laminated beam by the usage of a simulation-based design (SBD) which included several simulations and optimization techniques such as computer-aided design (CAD), finite element analysis (FEA), topology optimization (TO) and parametric optimization (PO). Their method had a two-stage optimization process. At first, traditional compliance TO using the SIMP approach, whereas, at the second stage, a PO with an evolutionary algorithm was applied.

Zhao Jing et al. [3] proposed a sequential permutation search (SPS) algorithm to optimize the stacking sequence of curved laminated composite shallow shells to achieve maximum fundamental frequency based on the developed Rayleigh-Ritz criterion. In their study, they

* Corresponding author. Tel.: +98-2173228974
E-mail address: rtalebi@iust.ac.ir

DOI: 10.22075/macs.2022.22219.1317
Received 2020-12-27; Received in revised form 2021-10-10; Accepted 2022-01-01.

allocated alike ply orientation at respective stacking positions and schemed the stacking sequence from internal to external positions consecutively. They also adjusted the bending-twisting coupling impacts of laminates through a sign optimization algorithm (SOA) which coupled in SPS.

Bertan Beylergil [4] performed an optimization on a hybrid composite laminate subjected to eccentric loading by the usage of a multi-objective genetic algorithm. He aimed to maximize the stiffness and minimize the cost and the weight of the composite structure, so he exploited a genetic aggregation model to generate the response surfaces and applied them to achieve the optimum design variables. In addition, he considered fiber orientations and the maximum Tsai-Wu failure index as design variables and constraints respectively.

Hozić et al. [5] suggested a novel discrete parametric methodology to optimize the topology and material of composite laminate structures, which is called Hyperbolic Function Parameterization (HFP). To allocate one design variable to each material candidate, a filtering technique based on hyperbolic functions was applied in HFP. Moreover, they assessed their methodology with other ones such as Discrete Material and Topology Optimization (DMTO) and Shape Function with Penalization (SFP) and demonstrated that despite the sensitivity of input parameters for the optimization problem, the performance of HFP is more consistent.

Wei et al. [6] proposed a two-level optimization strategy to fulfill optimization of symmetrical laminated composite cylindrical shells exposed to hydrostatic loading. At first, the best laminations with the maximum buckling pressure were estimated by coupling a conventional genetic algorithm (GA) with a finite element analysis optimization. Because of similar extensional stiffness coefficient ratios and bending stiffness coefficient ratios in this problem, at the second stage, a stiffness coefficient-based method (SCBM) was integrated with the GA to evaluate the lamination which stiffness coefficient ratios are closest to those found formerly.

Peng et al. [7] have rendered a multiple-scale uncertainty method to optimize stacking sequence and material patches of hybrid composite structures. In this study, they evaluated uncertainty propagation and performance based on classical laminated plate theory and also applied an adaptive neural network model to measure the uncertainties of the natural frequency, reliability index, and total cost. On the other hand, to maximize the natural frequency under constraints of the reliability index and total cost, the stacking sequences, and material patches were optimized through an adaptive genetic algorithm.

According to the road roughness, a sub-frame that is used to spread high loads over a wide chassis area is continuously under fatigue loading specified by altering the stress ratio, frequency, amplitude, and waveform of the cycling stresses. An optimum choice of fiber and matrix materials, fiber orientations, stacking sequence, and lamina thickness may substantially raise the fatigue life of a composite structure. Various researches have been performed to optimize composite structures under static loading to achieve the optimum fiber orientation but there are a few investigations to find out the optimal design of composites faced to variable loading.

Chanhui Lee et al. [8] presented an optimization approach to increase dynamic characteristics of patch-wise laminated composite used in ship structures. In their study, they present a two-level optimization strategy to progress the modal dynamic stiffness of laminated composite panels by the usage of lamination parameters and a patch-wise lay-up method.

Zhuo Chen et al. [9] submitted a new procedure for continuum topology optimization which has been able to perform based on fatigue-resistance design. In this method, penalized stress was chosen to circumvent the singularity issue and another additional penalization formulation of the elemental fatigue damage was proposed. To dealt with large-scale constraints, the p-norm function was assumed to gather all constraints into a single constraint.

Rajpal et al. [10] suggested a numerical method for optimization of a composite wing subjected to cyclic loading and evaluated fatigue impacts on the aeroelastic performance of the wing. In this study, an analytical fatigue model was used to reduce the moderation and exploit the potential of composite materials.

Kamaloo et al. [11] accomplished a delamination growth and thickness optimization of composite laminates under cyclic loading. They used NSGA-II to achieve a maximum delamination resistance and minimum thickness under fatigue loading. They also demonstrated that NSGA-II has good convergence with damage optimization in cracked glass/epoxy composite laminates.

So far, many fatigue theories such as stiffness and residual strength of investigated material have been established based on empirical and phenomenological modeling. One of the most primary models based on the S–N curve method was proposed by Hashin and Rotem [12]. They introduced the S–N curve for off-axis glass/epoxy samples with various orientations under a particular stress ratio. In this model, the static

strength was replaced by the fatigue strength failure criterion. In this way, they predicted the fatigue life of a UD composite in various directions of uni-axial loading. Reifsnider et al. [13] presented the critical element model based on micromechanical representations of the strength. Their theory was based upon suitable modeling of failure mechanisms regarding critical and sub-critical elements. The first one handled the failure process and specified the state of the material and the second one managed redistribution of internal stress and represented the changes in the local state of stress. This model can be utilized to estimate the life of composite laminates under random fatigue loading and the residual strength.

Diao et al. [14] established a statistical method for unidirectional composite laminate which was faced with multi-axial loading and the fatigue life was predicted respecting residual material characteristics deterioration rule. Lessard and Shokrieh [15-16] proposed a progressive model to estimate the fatigue life by using 3D finite element analysis. In their study, they applied experimental data for some fatigue characteristics such as longitudinal tensile, longitudinal compressive, transverse tensile, transverse compressive, and in-plane and out-of-plane shear. Cheng and Plumtree [17] and Shokrieh and Taheri-Behrooz [18] created similar fatigue damage parameters. This method was applied to unidirectional laminate because, in multidirectional ones, redistribution of the stress and strain would complicate the calculation of strain energy. So developing it into multidirectional laminates was difficult.

Recently, Haibin Tang et al. [19] studied the impression of fiber orientation on fatigue life diagram for Sheet Molding Compound composites. In the current study, the material behavior was considered for both quasi-static and cyclic loading conditions and they suggested a solution to correlate the fatigue life of the SMC material with a coefficient specified by the fiber orientation distribution. Moreover, they proposed a new model of fatigue life diagram which considered the effect of fiber orientation on the fatigue behavior of SMC composites.

Barbu et al. [20] proposed an authentic constitutive model to calculate the fatigue life of FRP composite confronted to longitudinal loads. The composite behavior was acquired through the serial/parallel mixing theory which was considered as a constitutive equation manager. The mentioned equation was joined with a load progressive strategy to decrease the time of calculation in simulations. Teimouri et al. [21] simulated mode 1 fatigue delamination growth in composites by coupling virtual crack closure technique (VCCT) and extended finite element method (XFEM) as XFEM-VCCT approach. Zhou et al. [22] introduced a fatigue progressive model which included delamination and in-plane damage. They evaluated in-plane fatigue life through fatigue master curves with various layup sequences under fatigue loading of different stress ratios. Furthermore, cohesive fatigue failure and Hashin failure criteria were applied to compute delamination and in-plane failure initiation, respectively.

Juiliang et al. [23] combined a Cohesive Zone Model and Regularized Extended Finite Element Method to simulate fatigue crack propagation in ABAQUS under cyclic or quasi-static loads. CZM model was able to estimate crack initiation and propagation through the relation between S-N and the Paris law. The major benefit of their model was the simple generation of S-N curves with few parameters and assumptions, while the experimental characterization of the Paris law parameters for all required stress ratios and material interfaces was very challenging and often infeasible.

Aoki et al. [24] suggested a methodology to assess fatigue progressive damage in composite laminates by the usage of inter-laminar and intra-laminar damages simulated via cohesive zone model and continuum damage mechanics, respectively. Gholami et al. [25] estimated elastic-plastic damage in the composite laminates. They coupled Continuum damage mechanics with the bridge micromechanics model to evaluate the fatigue damage and life for laminated composite structures. They applied a yield function to simulate the onset of plastic deformation and achieved evolution equations of the damage variables. At the next stage, the developed deformation plastic model was computed. Finally, a stochastic model was exploited to estimate the fatigue life of composite laminates. Bousfia et al. [26] proposed a novel model to calculate the fatigue life of a composite. They generated some curves which described the evolution of the deformation energy for diverse loading parameters based on their experimental works. These parameters depended on: amplitude load, maximum static load causing the rupture of the structure, and load ratio.

In the present work, the considered problem is the optimization of composite sub-frame subjected to cyclic load to achieve maximum fatigue life. The number and thickness of lamina are prescribed and fiber orientations are considered as optimization variables. A genetic algorithm is applied to find out the optimal stacking sequence of laminate to achieve the maximum fatigue life. Thus, by considering stress analysis and failure analysis, the fatigue life of a 3D epoxy carbon composite sub-frame is estimated by programming in ABAQUS.

2. Problem Statement

In this study, AS4/3501-4 laminate composite is considered and its characteristics are shown in table 1. Therefore, the problem is the design of the sub-frame subjected to cyclic load to achieve maximum fatigue life.

Fig. 1 represents different components of a rear suspension and inserted forces to the sub-frame. As shown in fig. 2, one end of the structure is fixed on the x, y, and z axes and another one fluctuates at the load ratio of 0.1 and frequency of 10 Hz. Figure 3 shows the load history; as presented in this figure, the minimum and maximum fatigue loads are 250 and 2500 N, respectively. Moreover, by considering the importance of safety in cars, a load factor of 2 is applied in this study. Therefore, the fatigue life of the composite sub-frame is determined based on the minimum and maximum cyclic loads of 500 and 5000N, respectively.

Table 1. Mechanical properties of AS4/3501-4

Mechanical Properties	Quantity
E_{11}(Gpa)	138
E_{22}= E_{33}(Gpa)	9
E_{12}= E_{13}(Gpa)	5.7
E_{23}(Gpa)	3
υ_{12}= υ_{13}	0.3
υ_{23}	0.42
δ	$1.015*10^{-8}$
X_T (Mpa)	2004
X_C (Mpa)	1197
Y_T = Z_T (Mpa	53
Y_C = Z_C (Mpa)	204
S_{12} = S_{13} (Mpa)	137
S_{23} (Mpa)	42

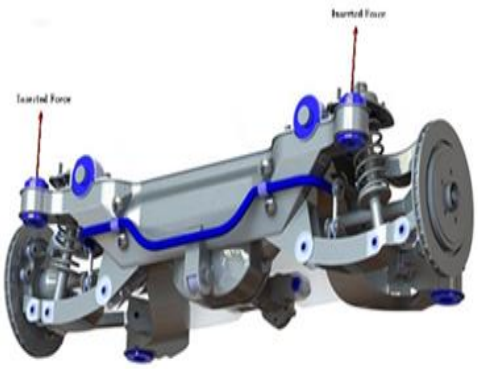

Fig. 1. Rear suspension

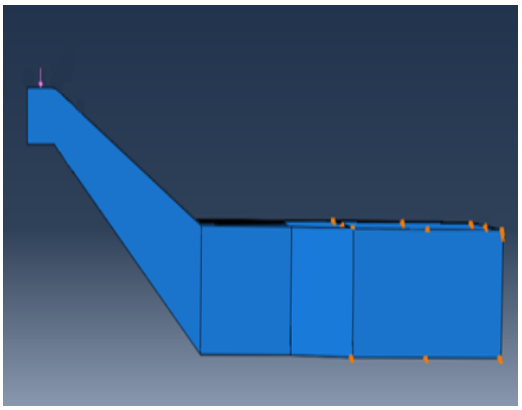

Fig. 2. Schematic of sub-frame

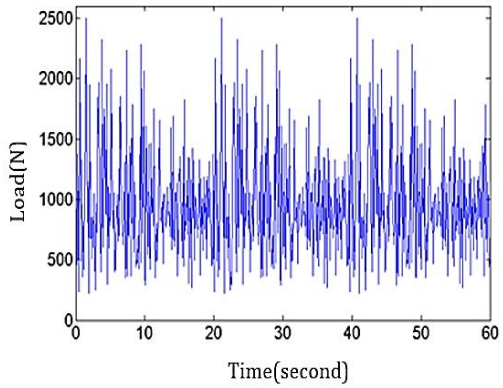

Fig. 3. The variable amplitude load-time history

3. Failure Criterion

In the present study, the 3D failure criterion of Lessard and Shokrieh [15-16] is utilized to diagnose the fatigue damage modes of a unidirectional ply subjected to different states of stress. This fatigue failure criterion was developed based on the Hashin-type static failure model and material characteristics are dependent to stress states, stress ratios, and the number of cycles.

In this model, 7 failure modes are considered and the impacts of substance nonlinearity on the fatigue failure criterion are taken into account. The first two modes demonstrate fiber tension and compression; the third failure mode represents the matrix/fiber shear failure. The fourth and the fifth are matrix failures in tension and compression. Finally, the sixth and the seventh ones are delaminations in tension and compression [15-16]. Regarding these failure modes, when the right hand of equations is greater than 1.0, failure occurs.

3.1. Fiber Tension Failure Mode

For fiber tension failure mode, the following equation is applied:

If $\sigma_{11}>0$,

$$FTT = \left(\frac{\sigma_{11}}{X_t(n.\sigma.r)}\right)^2 + \left(\frac{\frac{\sigma_{12}^2}{2E_{12}(n.\sigma.r)} + \frac{3}{4}\delta\sigma_{12}^4}{\frac{s_{12}^2}{2E_{12}(n.\sigma.r)} + \frac{3}{4}\delta\sigma_{12}^4}\right) + \left(\frac{\frac{\sigma_{13}^2}{2E_{13}(n.\sigma.r)} + \frac{3}{4}\delta\sigma_{13}^4}{\frac{s_{13}^2}{2E_{13}(n.\sigma.r)} + \frac{3}{4}\delta\sigma_{13}^4}\right) \quad (1)$$

X_t, S_{12}, and S_{13} imply residual tensile and shear strength, and E_{12} and E_{13} indicate the residual shear stiffness of UD ply. Also δ, r, n, and σ are substance nonlinearity parameters, stress ratio, number of cycles, and stress quantity, respectively.

3.2. Fiber Compression Failure Mode

In this failure mode, the next equation is utilized:

If $\sigma_{11}<0$,

$$FCF = \left(\frac{\sigma_{11}}{X_C(n.r.\sigma)}\right)^2 \quad (2)$$

X_c stands for the on-axis residual compressive strength.

3.3. Fiber-matrix Shear Failure Mode

For the third failure mode, the subsequent equation is applied:

If $\sigma_{11}< 0$,

$$FMFS = \left(\frac{\sigma_{11}}{X_c(n.\sigma.r)}\right)^2 + \left[\frac{\frac{\sigma_{12}^2}{2E_{12}(n.\sigma.r)} + \frac{3}{4}\delta\sigma_{12}^4}{\frac{S_{12}^2}{2E_{12}(n.\sigma.r)} + \frac{3}{4}\delta\sigma_{12}^4}\right] + \left[\frac{\frac{\sigma_{13}^2}{2E_{13}(n.\sigma.r)} + \frac{3}{4}\delta\sigma_{12}^4}{\frac{S_{13}^2}{2E_{13}(n.\sigma.r)} + \frac{3}{4}\delta\sigma_{13}^4}\right] \quad (3)$$

3.4. Matrix Tension Failure Mode

For this mode, the further equation is exploited:

If $\sigma_{22}> 0$,

$$MTF = \left(\frac{\sigma_{22}}{Y_t(n.\sigma.r)}\right)^2 + \left[\frac{\frac{\sigma_{12}^2}{2E_{12}(n.\sigma.r)} + \frac{3}{4}\delta\sigma_{12}^4}{\frac{S_{13}^2}{2E_{12}(n.\sigma.r)} + \frac{3}{4}\delta\sigma_{12}^4}\right] + \left[\frac{\sigma_{23}}{s_{23}(n.\sigma.r)}\right]^2 \quad (4)$$

S_{23} and Y_t are the residual shear strength and transverse residual tensile strength, respectively.

3.5. *Matrix Compression Failure Mode*

For the fifth failure mode, the following equation is utilized:

If $\sigma_{22}< 0$,

$$MCF = \left(\frac{\sigma_{22}}{Y_c(n.\sigma.r)}\right)^2 + \left[\frac{\frac{\sigma_{12}^2}{2E_{12}(n.\sigma.r)} + \frac{3}{4}\delta\sigma_{12}^4}{\frac{S_{13}^2}{2E_{12}(n.\sigma.r)} + \frac{3}{4}\delta\sigma_{12}^4}\right] + \left[\frac{\sigma_{23}}{s_{23}(n.\sigma.r)}\right]^2 \quad (5)$$

Y_c stands for the transverse residual compressive strength.

3.6. Delamination Tension Failure Mode

For the delamination tension mode, the subsequent equation is used:

If $\sigma_{33}> 0$,

$$DTF = \left(\frac{\sigma_{33}}{Z_t(n.\sigma.r)}\right)^2 + \left[\frac{\frac{\sigma_{13}^2}{2E_{13}(n.\sigma.r)} + \frac{3}{4}\delta\sigma_{13}^4}{\frac{S_{13}^2}{2E_{13}(n.\sigma.r)} + \frac{3}{4}\delta\sigma_{13}^4}\right] + \left[\frac{\sigma_{23}}{s_{23}(n.\sigma.r)}\right]^2 \quad (6)$$

Z_t signifies the normal residual tensile strength.

3.7. Delamination Compression Failure Mode

For the delamination compression mode, the following equation is exploited:

If $\sigma_{33}< 0$,

$$DCF = \left(\frac{\sigma_{33}}{Z_c(n.\sigma.r)}\right)^2 + \left[\frac{\frac{\sigma_{13}^2}{2E_{13}(n.\sigma.r)} + \frac{3}{4}\delta\sigma_{13}^4}{\frac{S_{13}^2}{2E_{13}(n.\sigma.r)} + \frac{3}{4}\delta\sigma_{13}^4}\right] + \left[\frac{\sigma_{23}}{s_{23}(n.\sigma.r)}\right]^2 \quad (7)$$

Zc implies the residual compressive strength.

4. Material Property Degradation

When a failure happens in an element according to previous failure criteria, material characteristics of the failed element are abruptly modified by a group of material property degradation rules. This type of deterioration implies "sudden" material property degradation. In this rule, just two kinds of aforementioned modes are catastrophic. Consequently, for the failed element under each mode of failure, a proper sudden material property degradation rule is considered. The material properties

degradation due to increasing the number of cycles is named ''gradual'' material property degradation.

4.1. Sudden Material Property Degradation Rule

In table 2 the abrupt material property degradation rules for a UD ply have been shown and explained in the following sections:

Table 2. Sudden material properties degradation rules

Failure mode	Failure index
Fiber tensile	$[E_{11}.E_{22}.E_{12}] \rightarrow [0.0.0]$ $[\nu_{12}.\nu_{21}.\nu_{13}.\nu_{31}.\nu_{23}.\nu_{32}] \rightarrow [0.0.0]$ $[S_{12}.S_{13}.S_{23}] \rightarrow [0.0.0]$ $[X_t.X_c.Y_t.Y_c] \rightarrow [0.0.0.0]$
Fiber compressive	$[E_{11}.E_{22}.E_{13}] \rightarrow [0.0.0]$ $[\nu_{12}.\nu_{21}.\nu_{13}.\nu_{31}.\nu_{23}.\nu_{32}] \rightarrow [0.0.0]$ $[S_{12}.S_{13}.S_{23}] \rightarrow [0.0.0]$ $[X_t.X_c.Y_t.Y_c] \rightarrow [0.0.0.0]$ $[S_{12}.S_{13}.S_{23}] \rightarrow [0.0.0]$
Fiber/matrix shear	$[E_{12}.\nu_{12}] \rightarrow [0.0]$ $[S_{12}] \rightarrow [0.0]$
Matrix tensile	$[E_{22}.\nu_{21}.\nu_{23}] \rightarrow [0.0.0]$ $[Y_t] \rightarrow [0]$
Matrix compression	$[E_{22}.\nu_{21}.\nu_{23}] \rightarrow [0.0.0]$ $[Y_c] \rightarrow [0]$
Delamination tension	$[E_{12}.\nu_{31}.\nu_{32}] \rightarrow [0.0.0]$ $[Z_t] \rightarrow [0]$
Delamination compression	$[E_{12}.\nu_{31}.\nu_{32}] \rightarrow [0.0.0]$ $[Z_c] \rightarrow [0]$

The first two failure modes are catastrophic for UD ply and the failed element cannot bear any kind of stress if one of these ruinous modes happens. Therefore, all mechanical properties of the failed ply diminish to zero. The second mode only impacts the matrix direction properties and is not catastrophic. For the fourth or the fifth failure modes, strength, stiffness, transverse modulus, and Poisson's ratio are decreased to ''virtual'' zero. When the laminate fails in the third mode, it cannot bear the in-plane shear load. So the load is transmitted to fiber or matrix direction. For the sixth and the seventh failure modes, normal strength, transverse stiffness, Poisson's ratio, and modulus are declined in a ''virtual'' zero [27].

4.2. Gradual Material Property Degradation Rule

Due to repetitive loading, the material properties of the laminate such as stiffness and strength of laminate dwindle. In the present essay, fatigue life is modeled by residual material property degradation theory which was established by Lessard and Shokrieh [15-16]. The experimental results of mechanical properties investigation on laminate showed primary growth of the longitudinal stiffness and strength [27]. Therefore, the residual strength and stiffness in the longitudinal direction of a UD ply under random loading and state of stress are calculated by the following equations:

$$R(n.r.\sigma) = [1 - N^a + cN^d(1-N)^e]^{\frac{1}{b}}(R_s - \sigma) \quad (8)$$

$$E(n.r.\sigma) - \sigma = [1 - N^a + cN^d(1-N)^e] \times \left(E_s - \frac{\sigma}{\varepsilon_f}\right) + \frac{\sigma}{\varepsilon_f} \quad (9)$$

$$N = \left(\frac{\log(n) - \log(0.25)}{\log(N_f) - \log(0.25)}\right) \quad (10)$$

in mentioned equations, R_s, E_s, R, E, and σ show static strength, static stiffness, residual strength, residual stiffness, and maximum applied stress severally. Also, n, ε_f, r, and N_f represent number of cycles, average strain to failure, stress ratio, and fatigue life. What is more, a, b, c, d, and e are experimental parameters for curve fitting and can be found in ref. [27].

For other directions, the residual strength and stiffness of a UD ply under random loading and state of stress are estimated by the following equations:

$$R(r.\sigma.n) = \left[1 - \left(\frac{\log(n) - \log(0.25)}{\log(N_f) - \log(0.25)}\right)^{\beta}\right]^{\frac{1}{\alpha}} \times (R_s - \sigma) + \sigma \quad (11)$$

$$E(r.\sigma.n) = \left[1 - \left(\frac{\log(n) - \log(0.25)}{\log(N_f) - \log(0.25)}\right)^{\lambda}\right]^{\frac{1}{\gamma}} \times \left(E_s - \frac{\sigma}{\varepsilon_f}\right) + \frac{\sigma}{\varepsilon_f} \quad (12)$$

α, β, γ, and λ are experimental parameters of curve fitting and can be found in ref [27].

5. Objective Function

In the present work, designing the stacking sequence of composite sub-frame subjected to cyclic loads is the considered problem. Each lamina includes 4 plies and the angle of each lamina is specified and there are 10 variables in the process. The purpose of this research is to maximize the fatigue life of composite sub-frame;

hence, the genetic algorithm has been developed to minimize the objective function. So the negative logarithm of fatigue life (–log (N_f)) is considered as the objective function.

Some experimental studies [28] showed that more than 45◦ discrepancy in the angles of two sequential laminae tends to delamination in laminates.

So if the difference between the fiber orientation angles of two sequential laminae generated by the genetic algorithm in the new configuration is greater than 45◦, a penalty function is added. Accordingly, the objective function is:

$$F = -\log(N) + \sum_{i=0}^{n} \eta(\Delta\theta - 45) \qquad (13)$$

where i demonstrates a set of laminae in which the restriction of angle difference is breached and η is the weighing factor.

6. Optimization Procedure

As indicated in fig. 4, at the beginning of the process, 100 primary laminate configurations are arbitrarily generated. The design variables are selected among 0◦, 15◦, 30◦, ±45◦, 60◦, 75◦, and 90◦. The fatigue life of lay-ups is determined according to fatigue failure criteria mentioned above by ABAQUS finite element software.

Then, their objective function values are calculated and sorted in descending. In the next step, crossover and mutation operators are used for creating new configurations and improving the results. For this purpose, an arithmetic crossover is used in this study. Based on the crossover rate, 80 configurations are randomly selected through the initial ones.

Then a random number such as α which is between 0 and 1, is generated and multiplied by each gene of the first parents, and (1-α) is multiplied by all of the genes from the second parents. Afterward, the two parents are summed. In this way, 40 new configurations are generated.

$$\begin{cases} Parents: (X_1.X_2 \ldots .X_n) and\ (Y_1.Y_2 \ldots .Y_n) \\ Child(\ new\ configs) = \alpha.\bar{X} + (1-\alpha).\bar{Y} \end{cases} \qquad (14)$$

If generated variables are greater than 90◦ or less than -45◦, the angles of 90◦ or -45◦ are replaced, respectively.

According to the mutation rate, some configurations are randomly selected. For each configuration (chromosome), one gene is randomly chosen. Then, the angle of this gene is changed among prescribed values and a new lay-up is created. The objective function is calculated for each new lay-up and sorted in descending.

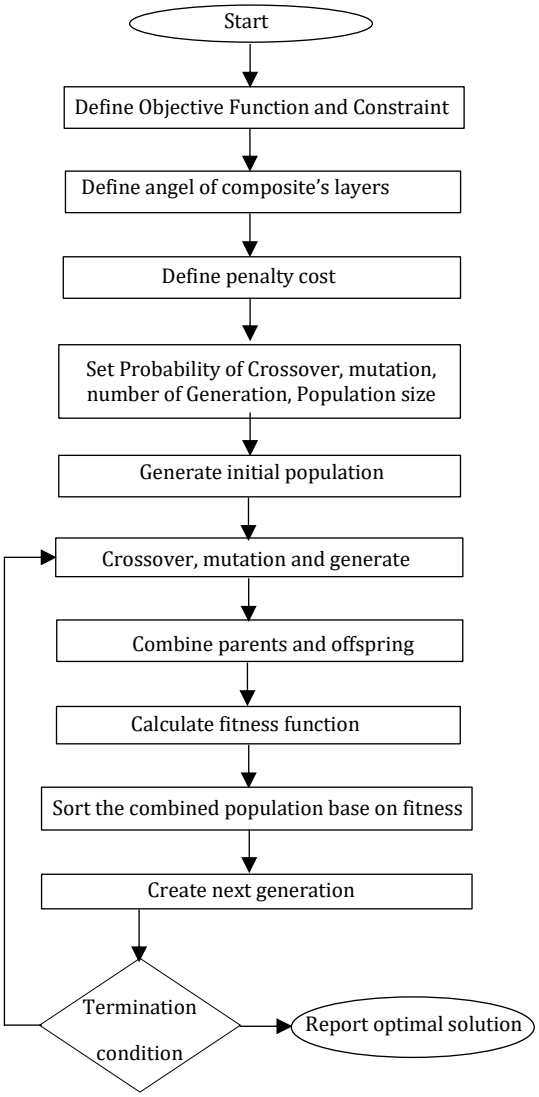

Fig. 4. Flowchart GA algorithm

Finally, the 100 configurations with the best value are selected as a new generation. This process continues till termination conditions are established. In this algorithm, termination conditions include:

- Setting the maximum number of repeated algorithms.
- Not entering a new solution to optimal solution set after several certain steps.

7. Numerical procedure

The optimization procedure was done by linking ABAQUS, FORTRAN, and MATLAB software. In this procedure, the orientation angles of laminae are generated within MATLAB and changed through a python file. Then, applied computational models for simulations are carried out in user subroutine UMAT of ABAQUS software which is recalled to each material

calculation item and explains particular material characteristics [29].

Furthermore, it updates the magnitudes of state variables and stresses at the end of the increment which is followed by the JACOBIAN matrix. Fiber orientations are specified for all elements according to the lay-up. UMAT is also utilized to compute the damage variable for each element and find out any failed element per fatigue algorithm. Failure status and damage are saved as variables for all elements during the whole stages of the algorithm. Eventually, the fatigue life of composite lay-up is determined. Then their objective function values are calculated within MATLAB.

8. Result and Discussion

The optimization algorithm was utilized to laminates of the sub-frame which had diverse lay-up configurations and subjected to prescribed load. Figure 5 shows the mean and the best solution schema during the optimization process. As shown both schemas have a downtrend. The best solution schema is not strictly decreasing and fixed in some points because of lying on the local optimal solution. This fix trend is broken and the decreasing trend is started again by mutation operation.

Mean solution schema which shows the mean of solutions has a smoother trend. Therefore, according to the results, the GA algorithm has a good performance. Finally, based on the results the sequence $[\pm 45_4/0_{12}]_s$ is determined as the best configuration. Figure 6 depicts delamination, matrix, and fiber failure damage evolutions in the critical element for $[\pm 45_4/0_{12}]_s$. It is shown that the element failed in matrix and delamination modes around 40% and 50% of total life, respectively, and variation can be seen in fiber failure mode about 50% of total life.

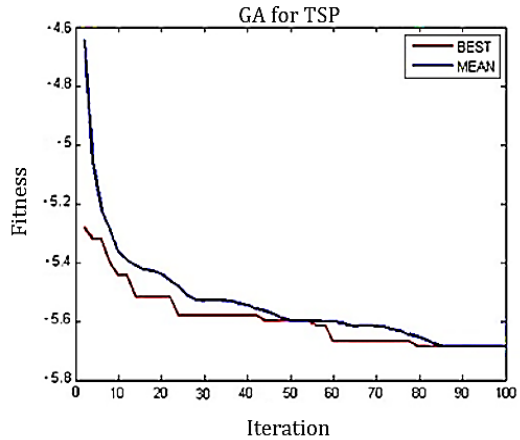

Fig. 5. Trend of the mean and the best solution in the optimization process

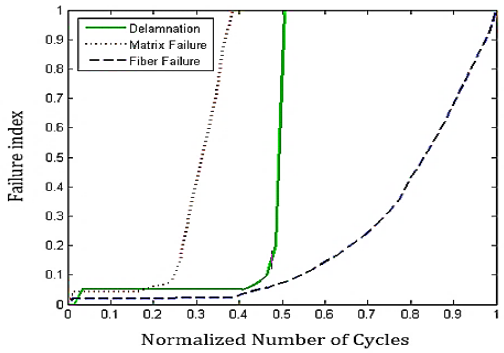

Fig. 6. Curves of delamination, matrix, and fiber failure damage evolutions in critical element for $[\pm 45_4/0_{12}]_s$

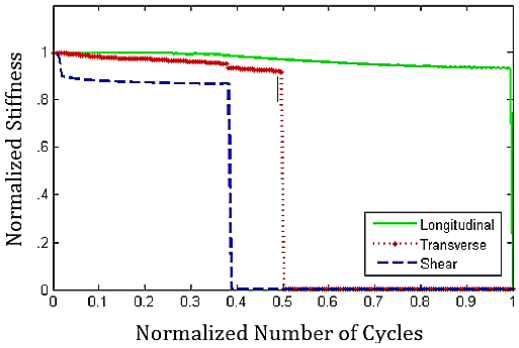

Fig. 7. Curves of normalized stiffness versus normalized life in longitudinal, transverse, and shear directions in the critical element for $[\pm 45_4/0_{12}]_s$.

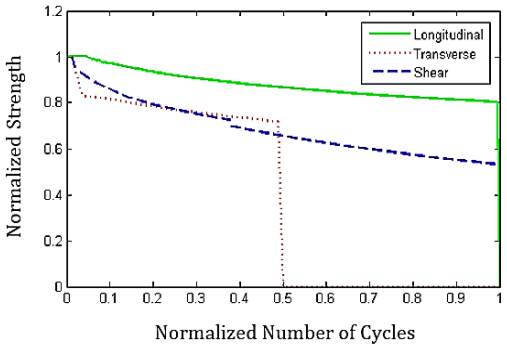

Fig. 8. Curves of the normalized strength versus normalized life in longitudinal, transverse, and shear directions in the critical element for $[\pm 45_4/0_{12}]_s$.

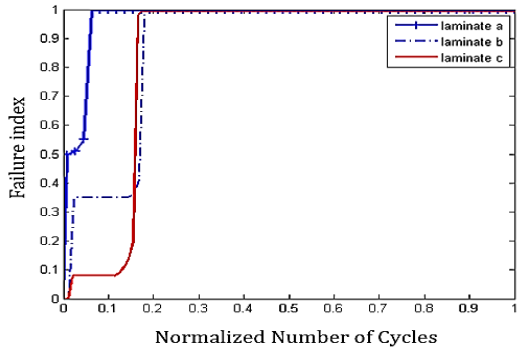

Fig. 9. Curves of the first failure in delamination mode for (a) $[04/90_{16}]_s$, (b) $[0_4/\pm 45_4/\pm 45_4]_s$, and (c) $[\pm 45_4/0_{12}]_s$ laminates.

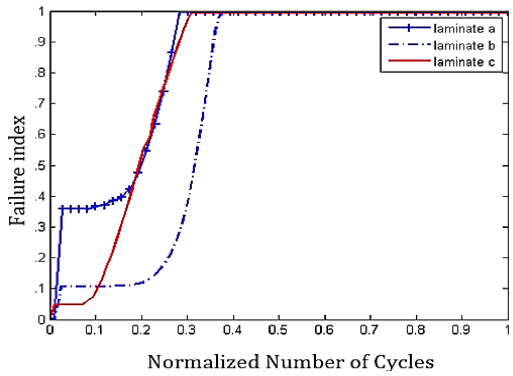

Fig. 10. Curves of the first failure in matrix mode for (a) $[04/90_{16}]_s$, (b) $[0_4/\pm45_4/\pm45_4]_s$, and (c $[\pm45_4/0_{12}]_s$ laminates.

Table 3. Fatigue life for different laminates and maximum von mises stress in their critical element

Lay up	Fatigue life (cycles)	Stress (MPa)
$[0_{40}]$	1940000	705
$[45_{40}]$	1560000	506
$[90_{40}]$	840000	470
$[0_4/90_{16}]_s$	1090000	400
$[0_4/\pm45_4/\pm45_4]_s$	1660000	335
$[0_4/30_4/\pm45_4/90_4]_s$	2210000	252
$[\pm45_4/0_{12}]_s$	3580000	315

Figures 7 and 8 show curves of normalized stiffness and strength versus normalized life, respectively in longitudinal, transverse, and shear directions. As presented in fig. 7, before failure, 7%, 8.55%, and 13% degradation happened in longitudinal, transverse, and shear stiffness respectively.

In addition, fig. 8 shows 20%, 23%, and 46% degradation in longitudinal, transverse, and shear strength. Concerning the failure modes, it can be seen that the mechanical properties were reduced in transverse and shear direction after failure. Therefore, after about 50% of total life, the load could not be sustained by the matrix. As the first and the second failure mode have been considered as the catastrophic modes, the loads were sustained by fibers until the longitudinal strength does not substantially decrease.

Table 3 shows fatigue life for different laminates and maximum von mises stress in their critical element. In unidirectional laminates, the configuration of $[0_{40}]$ has the greatest fatigue life and sequence $[90_{40}]$ has the lowest one. Hence $[0_{40}]$ laminate has more fatigue life as well as it could carry more stress than $[90_{40}]$ one.

Figures 9 and 10 show the first failure in matrix and delamination modes for $[0_4/90_{16}]_s$, $[0_4/\pm45_4/\pm45_4]_s$, $[0_4/30_4/\pm45_4/90_4]_s$ and $[\pm45_4/0_{12}]_s$ laminates. Low mechanical properties of 90◦ ply and the considerable difference between the angles of 0° and 90° layers were led to degradation of the laminate, as the first delamination occurs about 6% of total life.

On the other hand, usage of 90◦ layers as consecutive plies was tended to the progression of matrix damage through the thickness and conduct major matrix cracks. Also, 90° layers in the configuration were ended up growing the stress in the sub-frame and because of low strength, subsequently, the failure happened in fiber mode. As figs. 9 and 10 depict, the lower angular differences and mechanical properties between 0° and ±45° were caused less stress on the sub-frame. In contrast, usage of ±45° layers was led to restrain crack propagation in laminate and postpone the first matrix failure. Besides, the application of ±45° layers as outer ones were triggered by a rise in stiffness, toughness, and impact resistance of laminate.

9. Conclusion

In this study, an optimization method was proposed to find out the optimal sequence of composite sub-frame subjected to fatigue load achieving maximum fatigue life. The fiber orientation angle in each lamina was considered as a variable to achieve this purpose. The model developed by Lessard and Shokrieh was applied to establish the fatigue life of the configurations produced during optimization. In this process, 100 initial configurations were randomly generated and 100 iterations were done to find the optimum orientation. According to the results, $[\pm45_4/0_{12}]_s$ laminate was determined as the best orientation.

It can be seen that after failure in delamination and matrix modes, mechanical properties were reduced in the transverse and shear direction. Therefore, the matrix could not bear the load and fibers were responsible to carry the load. These failures were led to rising stress on the sub-frame until the catastrophic failure mode happened. The difference in angular and mechanical properties between layers caused to degradation of the laminate, as the first failure occurred at the initial stage of the fatigue life. Usage of 90° layers as consecutive plies were tended to the progression of matrix damage and 90° layers in the configuration were led to growing stress.

Furthermore, the lower angular difference and mechanical properties between 0° and ±45° resulted in less stress and so the first matrix failure was postponed. Usage of ±45° as outer layers were caused to increase the stiffness, toughness, and impact resistance of laminate.

Nomenclature

E_{11}	Longitudinal modulus of elasticity
E_{22}	Transverse modulus of elasticity
E_{33}	Normal modulus of elasticity
G_{12}, G_{13}, G_{23}	Shear modulus of elasticity
n	Number of cycles
N_f	Number of the cycle at failure
R	Residual strength
Rs	Static strength
E	Residual stiffness
Es	Static stiffness
r	Stress ratio
S_{12}, S_{13}, S_{23}	Shear strength
X_t	Longitudinal tensile strength
Xc	Longitudinal compression strength
Y_t	Transverse tensile strength
Y_c	Transverse compression strength
Z_t	Normal tensile strength
Z_c	Normal compression strength
δ	Material nonlinearity
υ_{ij}	Poisson's ratio
$\sigma_{ij}\,(\tau_{ij})$	Stress components
$\mathcal{E}_f$	Average strain to failure
F	objective function
η	Weighting factor
θ	Fiber orientation angle
α	A random number between 0 and 1

References

[1] Franz, M., Schleich, B. and Wartzack, S., 2019. Influence of layer thickness variations on the structural behaviour of optimised fibre reinforced plastic parts. *Procedia CIRP*, *85*, pp.26-31.

[2] Tyflopoulos, E., Hofset, T.A., Olsen, A. and Steinert, M., 2021. Simulation-based design: A case study in combining optimization methodologies for angle-ply composite laminates. *Procedia CIRP*, *100*, pp.607-612.

[3] Jing, Z., Sun, Q., Zhang, Y., Liang, K. and Li, X., 2021. Stacking sequence optimization of doubly-curved laminated composite shallow shells for maximum fundamental frequency by sequential permutation search algorithm. *Computers & Structures*, *252*, p.106560.

[4] Beylergil, B., 2020. Multi-objective optimal design of hybrid composite laminates under eccentric loading. *Alexandria Engineering Journal*, *59*(6), pp.4969-4983.

[5] Hozić, D., Thore, C.J., Cameron, C. and Loukil, M., 2021. A new method for simultaneous material and topology optimization of composite laminate structures using Hyperbolic Function Parametrization. *Composite structures*, *276*, p.114374.

[6] Wei, R., Pan, G., Jiang, J., Shen, K. and Lyu, D., 2019. An efficient approach for stacking sequence optimization of symmetrical laminated composite cylindrical shells based on a genetic algorithm. *Thin-Walled Structures*, *142*, pp.160-170.

[7] Peng, X., Qiu, C., Li, J., Wu, H., Liu, Z. and Jiang, S., 2021. Multiple-scale uncertainty optimization design of hybrid composite structures based on neural network and genetic algorithm. *Composite Structures*, *262*, p.113371.

[8] Lee, C., Greenhalgh, E.S. and Panesar, A., 2021. Optimization of patch-wise laminated composite panels for enhanced dynamic characteristics. *Composite Structures*, *269*, p.114017.

[9] Chen, Z., Long, K., Wen, P. and Nouman, S., 2020. Fatigue-resistance topology optimization of continuum structure by penalizing the cumulative fatigue damage. *Advances in Engineering Software*, *150*, p.102924.

[10] Rajpal, D., Mitrotta, F.M.A., Socci, C.A., Sodja, J., Kassapoglou, C. and De Breuker, R., 2021. Design and testing of aeroelastically tailored composite wing under fatigue and gust loading including effect of fatigue on aeroelastic performance. *Composite Structures*, *275*, p.114373.

[11] Kamaloo, A., Jabbari, M., Tooski, M.Y. and Javadi, M., 2019. Optimization of thickness and delamination growth in composite laminates under multi-axial fatigue loading using NSGA-II. *Composites Part B: Engineering*, *174*, p.106936.

[12] Harris, B., 1977. Fatigue and accumulation of damage in reinforced plastics. *In SEE fatigue Group Conference on fatigue of FRP, London*.

[13] Reifsnider, K., Stinchcomb, W., 1986. A critical-element model of the residual strength and life of fatigue loaded composite coupons. *Composite Materials: Fatigue and Fracture,* pp.298-313.

[14] Diao, X., Lessard, L.B. and Shokrieh, M.M., 1999. Statistical model for multiaxial fatigue behavior of unidirectional plies. *Composites science and technology*, *59*(13), pp.2025-2035.

[15] Shokrieh, M.M. and Lessard, L.B., 1997. Multiaxial fatigue behaviour of unidirectional plies based on uniaxial fatigue experiments—II. Experimental evaluation. *International journal of fatigue*, *19*(3), pp.209-217.

[16] Shokrieh, M.M. and Lessard, L.B., 2000. Progressive fatigue damage modeling of composite materials, Part II: Material characterization and model verification. *Journal of Composite materials*, *34*(13), pp.1081-1116.

[17] Plumtree, A. and Cheng, G.X., 1999. A fatigue damage parameter for off-axis unidirectional fibre-reinforced composites. *International Journal of fatigue*, *21*(8), pp.849-856.

[18] Shokrieh, M.M. and Taheri-Behrooz, F., 2006. A unified fatigue life model based on energy method. *Composite Structures*, *75*(1-4), pp.444-450.

[19] Tang, H., Chen, Z., Zhou, G., Sun, X., Li, Y., Huang, L., Guo, H., Kang, H., Zeng, D., Engler-Pinto, C. and Su, X., 2019. Effect of fiber orientation distribution on constant fatigue life diagram of chopped carbon fiber chip-reinforced Sheet Molding Compound (SMC) composite. *International Journal of Fatigue*, *125*, pp.394-405.

[20] Barbu, L.G., Oller, S., Martinez, X. and Barbat, A.H., 2019. High-cycle fatigue constitutive model and a load-advance strategy for the analysis of unidirectional fiber reinforced composites subjected to longitudinal loads. *Composite Structures*, *220*, pp.622-641.

[21] Teimouri, F., Heidari-Rarani, M. and Aboutalebi, F.H., 2021. An XFEM-VCCT coupled approach for modeling mode I fatigue delamination in composite laminates under high cycle loading. *Engineering Fracture Mechanics*, *249*, p.107760.

[22] Zhou, S., Li, Y., Fu, K. and Wu, X., 2021. Progressive fatigue damage modelling of fibre-reinforced composite based on fatigue master curves. *Thin-Walled Structures*, *158*, p.107173.

[23] Liang, Y.J., Dávila, C.G. and Iarve, E.V., 2021. A reduced-input cohesive zone model with regularized extended finite element method for fatigue analysis of laminated composites in Abaqus. *Composite Structures*, *275*, p.114494

[24] Aoki, R., Higuchi, R. and Yokozeki, T., 2021. Fatigue simulation for progressive damage in CFRP laminates using intra-laminar and inter-laminar fatigue damage models. *International Journal of Fatigue*, *143*, p.106015.

[25] Gholami, P., Farsi, M.A. and Kouchakzadeh, M.A., 2021. Stochastic fatigue life prediction of Fiber-Reinforced laminated composites by continuum damage Mechanics-based damage plastic model. *International Journal of Fatigue*, *152*, p.106456.

[26] Mohammed, B., Mohamed, A. and Brahim, O., 2021. Fatigue life prediction of composite laminate under random loading service: An energy approach. *Materials Today: Proceedings*, *36*, pp.29-33.

[27] Naderi, M. and Maligno, A.R., 2012. Fatigue life prediction of carbon/epoxy laminates by stochastic numerical simulation. *Composite Structures*, *94*(3), pp.1052-1059.

[28] Irisarri, F.X., Bassir, D.H., Carrere, N. and Maire, J.F., 2009. Multiobjective stacking sequence optimization for laminated composite structures. *Composites Science and Technology*, *69*(7-8), pp.983-990.

[29] Nikishkov, Y., Makeev, A. and Seon, G., 2013. Progressive fatigue damage simulation method for composites. *International Journal of Fatigue*, *48*, pp.266-279.